Two-Wavelength Holographic Measurement of Temperature and Concentration During Alloy Solidification

A. Ecker*
NASA Marshall Space Flight Center, Huntsville, Alabama

Simultaneous measurement of the temperature and concentration distribution within a fluid can be made using a "two-wavelength holographic" setup. The technique is successfully applied to the study of temperature, concentration, and flowfields in the melt of a transparent "model alloy" during solidification.

Nomenclature

c	= concentration
g	= acceleration due to gravity
h_z	= height of sample
l	= sample depth
M	= interference order
$n(T,c,\lambda)$	= refractivity
$R(\lambda)$	= refraction index
s	= optical path length
t	= time, s
T	= temperature
y	= coordinate
$\lambda(T,c)$	= wavelength
$\rho(T,c)$	= density, g/cm^3

Introduction

INTERFEROMETRIC techniques are helpful tools for fundamental investigations of the fluid flow, temperature, and concentration distribution in front of a solidifying interface. These effects change the solidification conditions of cast metallic materials; hence, they influence their microstructure. In order to optimize the properties of the castings, comprehensive knowledge is required of the interaction between the fluid flow in the melt and the temperature- and concentration-dependent layers close to the solidification front. Transparent model systems that solidify in the same manner as metals can be effectively utilized for fundamental investigations because they allow in situ observation and interferometric measurement of the environment close to the solid/liquid interface.[1-3]

The objective of this work is to describe a new method for simultaneous measurements of the interaction between the temperature and concentration distribution and the fluid flow in the melt of different g environments adjacent to the solid/liquid interface in metallic alloys using transparent solidifying monotectic model systems. The "two-wavelength holographic" method provides the opportunity for direct measurement of temperature and concentration.

Transparent Monotectic Model Systems

In order to examine the fluid flow in melts, transparent model systems that solidify in the same manner as metals are studied. Figure 1 shows a growing dendritic interface of the succinonitrile-ethanol model system.[1,2,4]

Since the dendritic structure is strongly dependent on the fluid flow conditions in the melt (Fig. 2),[1,2] the influence on the physical properties of the cast metallic material has to be considered.

Figure 3 shows one principal phase diagram of the two studied monotectic[5] model systems: succinonitrile-ethanol and succinonitrile-water.

Fluid Flow Conditions in the Melt of a Solidifying Monotectic Alloy

The fluid flow in the melt in front of a solidifying monotectic alloy will be driven by either thermocapillary or buoyancy forces. The causes of fluid flow in monotectic systems in the vicinity of the solidification front during ground-based laboratory experiments are summarized as[3]

1) Separation processes below the consolute temperature.

2) Dynamic processes at the liquid-liquid-solid (L_1-L_2-S_1) trijunction (wetting conditions).

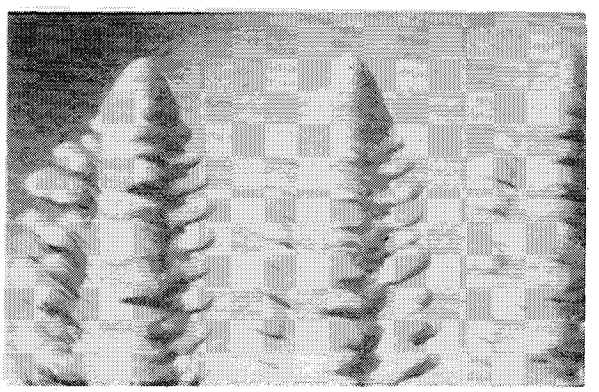

Fig. 1 Growth of single dendrites in the organic transparent succinoitrile-ethanol model system.[1,2]

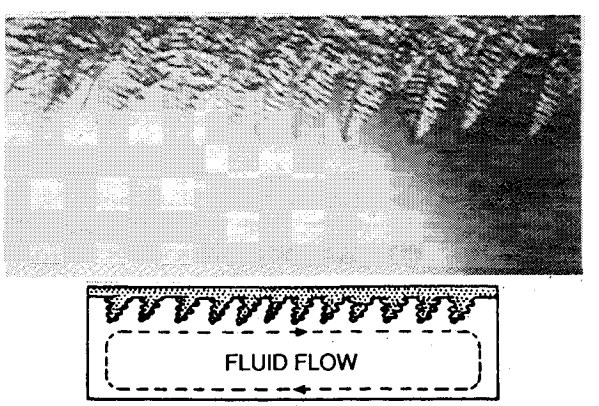

Fig. 2 Trunk of the dendrites grows with an angle against the direction of the fluid flow in the melt. The symmetrical dendritic tip growth will be changed by fluid flow conditions.

Received Nov. 20, 1986; presented as Paper 87-0579 at the AIAA 25th Aerospace Sciences Meeting, Reno, NV, Jan. 12-15, 1987; revision received March 2, 1987. Copyright © American Institute of Aeronautics and Astronautics, Inc., 1987. All rights reserved.

*European Space Agency Visiting Scientist.

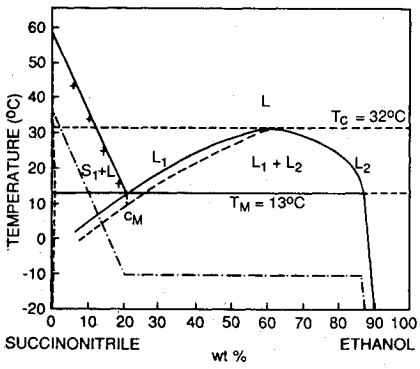

Fig. 3 Phase diagram of the monotectic succinonitrile-ethanol model allow based on measurements by Schreinemakers[4] and Ecker.[1]

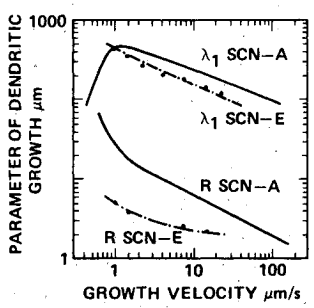

Fig. 4 Primary dendritic spacing and the tip radius measured at the succinonitrile-ethanol system[1,2] in comparison with the data measured by Somboonsuk et al.[6] at the system succinonitrile-aceton.

3) Solidification velocity (incorporating or pushing of droplets).

4) Thermocapillary-driven motion resulting from thermal and solutal differences in the interface.

5) Density differences between the liquid-liquid (L_1-L_2).

Two-Wavelength Holographic Techniques

For the basic understanding of the fluid flow in the melt in front of a solidifying interface, optical measurements can be made using microscopy or shadowgraph techniques. This provides in situ information about the fluid flow conditions and the parameters of the solidification front dynamics (e.g., primary dendrite spacing and dendrite tip radius; see Fig. 4). The fluid motion can be discerned from changes of refractivity or moving particles. These techniques cannot provide information about the temperature and concentration distribution and their interaction with the fluid flow in the melt.

A first experiment using such techniques to determine the concentration and temperature distribution in the monotectic system at 1 *g* and microgravity involved the hypomonotectic system of succinonitrile-ethanol.[1-3] The particular technique employed was Ganzfeld differential interferometry[7] in conjunction with thermocouples placed in the melt. A development of a local concentration maximum was revealed in the melt at 1 *g*. In comparison, reduced gravity conditions, such as those which prevailed during the sounding rocket experiment TEXUS-10,[1,2,8] lead to concentration boundary layers ahead of the solidification front (Fig. 5). Under microgravity conditions, the temperature profile depends only on diffusion. Under 1 *g*, the temperature profile differs from the pure thermodiffusion profile. Also, small rising droplets, which will be resolved at the critical temperature (T_c = 32°C), change the temperature and concentration profiles in the melt. A concentration maximum was found at the 32°C isotherm in the melt. With interferometric techniques of this kind, only those disturbances large enough (e.g., large migrating droplets or rising volumes) to induce refractivity changes greater than the minimum interferometric resolution can be detected. Droplets of the necessary size appear only because of the decomposition phenomenon

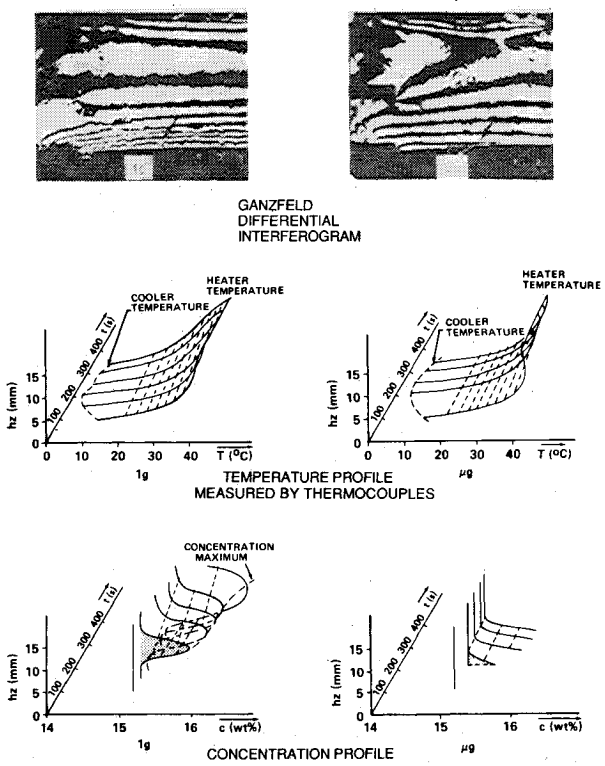

Fig. 5 Concentration and temperature profile of the 1 *g* and microgravity TEXUS-10 experiment "boundary layers at transparent solidifying melts" with SCN-E. The concentration layer in front of the solid-liquid interface corresponds to the well-known theory ($\delta_c \sim 2 \cdot D/v$).[9]

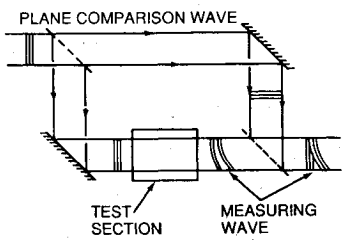

Fig. 6 Optical setup of a Mach-Zehnder interferometric system.[10]

and Ostwald ripening in the melt or the monotectic solidification process at lower solidification rates.

A Mach-Zehnder interferometric technique (Fig. 6) used to measure concentration and temperature in front of a solid/liquid interface provides information only about the refractivity changes in the melt. Since the refractivity is a function of the temperature and concentration, there has to be additional information on temperature or concentration distribution in the melt in order to evaluate the interferograms.

Until now interferometric measurements in front of solidifying melts relied upon the simultaneous use of thermocouples in the melt. Unfortunately, this provides only local information about the temperature profile. The nature of the temperature profile measured by thermocouples (TEXUS-10: six 3 m thermocouples in the sample) is uncertain since it is necessary to assume a spatial linear temperature distribution in the melt. Temperature changes in the melt resulting from fluid flow are, using a standard interferometric technique, not only undetectable but cause a misinterpretation of the concentration distribution, since the concentration distribution in the melt is calculated from the density profile on the basis of the measured temperatures.

Only the two-wavelength holographic technique provides the possibility of a separate measurement of temperature and concentration profiles without the use of thermocouples in the melt. The accuracy of the refractivity measurements is as high

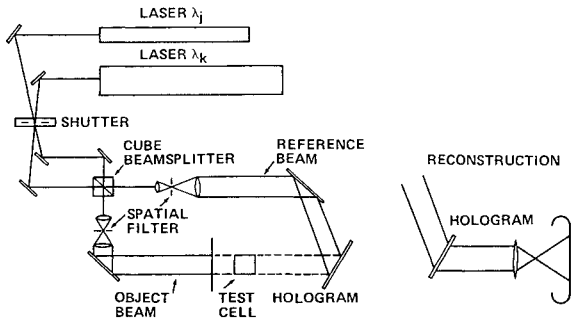

Fig. 7 Principal setup for the two-wavelength holographic device, first used by El-Wakil and Ross.[11]

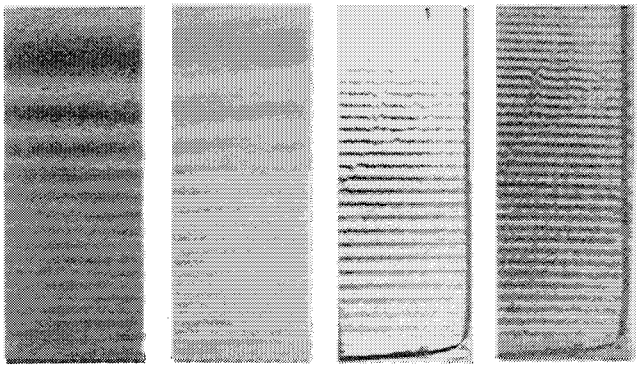

a) He-Ne Argon b) He-Ne Argon

Fig. 8 Reconstruction of a two-wavelength hologram using a He-Ne and an argon laser. Both reconstructions show: a) the same temperature changes, and b) the same concentration changes. The number of fringes observed differs about 34%.

as that obtained using standard holographic technology. The two-wavelength holographic method is transferable to any holographic system (Fig. 7). This technique was first used by Mayinger and Panknin[10] and El-Wakil and Ross[11] to measure the temperature and concentration of a burning fuel drop. The technique offers a significant opportunity to determine the temperature and concentration profiles simultaneously in all processes where heat and mass transport in transparent systems occurs. The technique is based on the simultaneous recorded images of both wavelengths on one holographic plate. Each hologram is reconstructed separately for each wavelength and contains the information on temperature and concentration changes. Since the refractivity is also a function of the wavelength,[10,11] it is possible to determine both profiles from the differences between both holograms (Fig. 8).

Initial information obtained from the holograms represent changes in the optical path length s through the sample via the equation

$$M\lambda = \int_s (n_1 - n_2)\, \mathrm{d}s \qquad (1)$$

where M is the interference order in multiples of the different wavelengths λ_j and λ_k and n the refractivity. Equation (1) can be integrated if the intensity of the total field is constant. For fluids, the Lorentz-Lorenz equation gives the relation between the refractivity n, refractive index R, and density ρ of the melt,

$$\frac{n(T,c)^2 - 1}{n(T,c)^2 + 2} = R(\lambda) \cdot \rho(T,c) \qquad (2)$$

The slope of the fringe shift $\mathrm{d}M/\mathrm{d}y$ depends on the change of the refractivity between both exposures. Since the information of the refractivity changes due to temperature and concentration variation is in both reconstructions, it is possible to elimi-

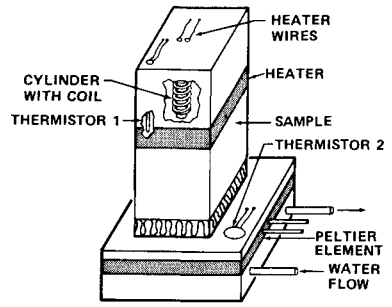

Fig. 9 Sample[12] for the use in the optical setup.

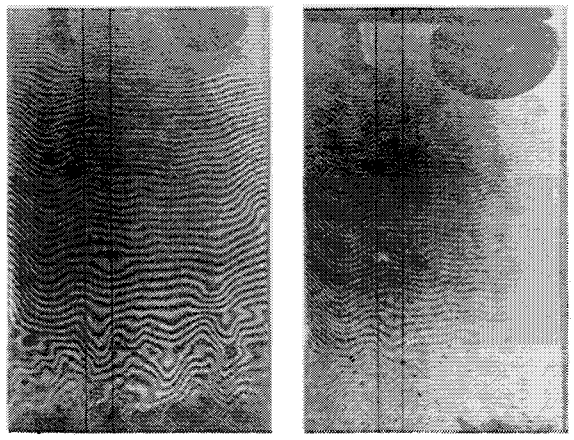

He-Ne Argon

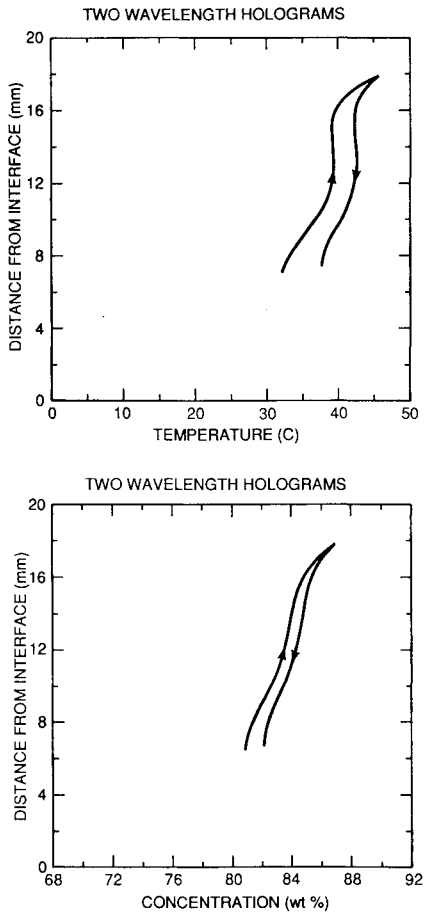

Fig. 10 Two-wavelength holography provides the possibility of separating temperature and concentration profiles in the melt at different cuts.

nate the concentration and solve it for the temperature profile,

$$\frac{dT}{dy} = \frac{\frac{\partial n_k}{\partial c} \cdot \frac{dM_j}{dy} \cdot \frac{\lambda_j}{l} - \frac{\partial n_j}{\partial c} \cdot \frac{dM_k}{dy} \cdot \frac{\lambda_k}{l}}{\frac{\partial n_k}{\partial c} \cdot \frac{\partial n_j}{\partial T} - \frac{\partial n_k}{\partial T} \cdot \frac{\partial n_j}{\partial c}} \tag{3}$$

with l as the sample depth, λ the wavelength ($\lambda_j = 488$ nm, $\lambda_k = 632.8$ nm), n the refractivity $f(\lambda,T,c)$, c the concentration, and T the temperature.

Using the temperature profile from Eq. (3), the concentration profile may be determined by

$$\frac{dc}{dy} = \frac{(dM_k/dy) \cdot (\lambda_k/l) - (\partial n_k/\partial T) \cdot (dT/dy)}{(\partial n_k/\partial c)} \tag{4}$$

To achieve a sufficient difference at the wavelength-dependent refractivities, lasers have to be selected with a large wavelength difference.

Two-Wavelength Holographic Setup

Using the same optical path as a normal holographic setup, a second laser was added, as shown in Fig. 7. For ground-based measurements, a He-Ne ($\lambda = 632.8$ nm) and an argon ($\lambda = 488$ nm) laser were chosen. Because of the high power consumption of an argon laser, another laser type had to be selected for the planned reduced-gravity experiments (10^{-2} g) achieved during parabolic flight trajectories (KC-135). Therefore, a He-Cd ($\lambda = 422$ nm) laser was selected with a coherence length larger than 100 mm. A glass cell (Fig. 9) was used with Peltier cooling at the lower side and resistance heating at the top side. The temperature at both sides was controlled by thermocouples.

If both lasers are carefully aligned, spatial filters with a hole of 25 μm may be used. In the laboratory, the needed power output of the argon laser is 20 mW compared to 10 mW output of the He-Ne laser. One reason for this large difference is that the holographic material (10E75) is 60% less sensitive at 488 nm (argon laser) than at 632.8 nm (He-Ne laser). Using a He-Ne and a He-Cd laser (442 nm), the sensitivity of the holographic material is identical for both wavelengths.

For the evaluation of the two-wavelength holographic holograms, the change of refractivity has to be determined as a function of wavelength, temperature, and concentration. First, the refractivity was determined using an Abbe refractometer. These data were proved by holographic measurements of the fringe shift due to a stable temperature gradient in the melt. The holograms can be evaluated for two-dimensional fluid flow in the melt using an image analyzing system. Figure 10 shows the temperature and concentration profiles in front of a solid/liquid interface of the succinonitrile-water system.

Discussion

An improvement of this two-wavelength holographic technique would be the use of a third wavelength. This would have two advantages: 1) the third laser would allow an increase in the measurement accuracy because of a three-point measurement and 2) the third laser would be a good safety margin for use under migrogravity conditions (Shuttle or space station) due to the possibility of getting results if only two lasers were operating.

Acknowledgments

The author gratefully acknowledges P. R. Sahm for providing the opportunity to initiate this research and for his support during his Ph.D. work at the Foundry Institute of the University of Aachen, the European Space Agency for continuing to support this research, and NASA for making the experimental facilities available.

References

[1]Ecker, A., "Erstarrungsfrontdynamik in Durchsichtigen Modellsystemen," Dissertation, University of Aachen (RWTH), Aachen, FRG, 1985.

[2]Ecker, A. and Sahm, P. R., "Erstarrungsfrontdynamische Messungen am monotektischen Modellsystem Bernsteinsaure dinitrilethanol," *Giessereiforschung*, Vol. 39, No. 1, 1987.

[3]Ecker, A., Alexander, J. I. D., and Frazier, D. O., "Fluid Flow in the Melt of Solidifying Monotectic Alloys," *Metallurgical Transactions* (submitted for publication).

[4]Schreinemakers, F. A. H., "Gleichgewichte im System: Wasser, Alkohol, Bernsteinsäuredinitril," *Zeitschrift für Physikalische Chemie*, Vol. 26, 1898, p. 958.

[5]Grugel, R. N. and Hellawell, A., "The Solidification of Monotectic Alloys—Microstructures and Phase Spacings," *Metallurgical Transactions*, Vol. 15A, 1984, p. 1626.

[6]Somboonsuk, K., Mason, J. T., and Trivedi, R., "Interdendritic Spacing: Part I. Experimental Studies," *Metallurgical Transactions*, Vol. 15A, 1984, p. 968.

[7]Oertel, H., Jr. and Jaeger, W., "Optik Workshop, Ausblick auf die Anwendung des Weltraum-Optiklabors," *BMFT Mitteilungen*, Rept. W-79 Weltraumforschung, 1979, p. 119.

[8]Sahm, P. R. and Ecker, A., "Stadium von Gefügebildungsprozessen an transparenten Modellsystemen," *Zeitschrift für Metallkunde*, Vol. 75, No. 5, 1984, p. 325.

[9]Kurz, W. and Fisher, D. J., *Fundamentals of Solidification*, Trans. Tech. Pub., Aedermannsdorf, Switzerland, 1984, p. 241.

[10]Mayinger, F. and Panknin, W., "Holography in Heat and Mass Transfer," *Proceedings of the 5th International Heat Transfer Conference*, Tokyo, 1974, p. 28.

[11]El-Wakil, M. M. and Ross, P. A., "A Two Wavelength Interferometric Technique for the Study of Vaporization and Combustion on Fuels, Liquid Rockets and Propellants," *AIAA Progress in Astronautics and Rocketry: Liquid Rockets and Propulsion*, Vol. 2, edited by L. E. Bollinger, M. Goldsmith, and A. W. Lemmon Jr., Academic Press, New York, 1960.

[12]Facemire, B. R., private communication, 1986.